Mathematical Biosciences 241 (2013) 49–55

Contents lists available at SciVerse ScienceDirect

Mathematical Biosciences

journal homepage: www.elsevier.com/locate/mbs

A mathematical model for coupling within-host and between-host dynamics in an environmentally-driven infectious disease

Zhilan Feng [a,*], Jorge Velasco-Hernandez [b], Brenda Tapia-Santos [c]

[a] Department of Mathematics, Purdue University, West Lafayette, USA
[b] Programa de Matemáticas Aplicadas y Computación, Instituto Mexicano del Petróleo, Mexico
[c] Facultad de Matemáticas, Universidad Veracruzana, Mexico

ARTICLE INFO

Article history:
Received 1 April 2012
Received in revised form 10 September 2012
Accepted 15 September 2012
Available online 4 October 2012

Keywords:
Toxoplasma gondii
Multiple time scales
Between-host dynamics
Within-host dynamics
Reproduction numbers
Backward bifurcation

ABSTRACT

This work presents a new model for the linking of within- and between-host dynamics. We use this as a conceptual model for the dynamics of *Toxoplasma gondii*, in which the parasite's life cycle includes interactions with the environment. We postulate the infection process to depend on the size of the infective inoculum that susceptible hosts may acquire by interacting with a contaminated environment. Because the dynamical processes associated with the within- and between-host occur on different time scales, the model behaviors can be analyzed by using a singular perturbation argument, which allows us to decouple the full model by separating the fast- and slow-systems. We define new reproductive numbers for the within-host and between host dynamics for both the isolated systems and the coupled system. Particularly, the reproduction number for the between-host (slow) system dependent on the parameters associated with the within-host (fast) system in a very natural way. We show that these reproduction numbers determine the stability of the infection-free and the endemic equilibrium points. Our model may present a so-called backward bifurcation.

1. Introduction

For most infectious diseases there are two key processes in the host-parasite interaction. One is the epidemiological process associated with the disease transmission, and the other is the immunological process at the individual host level. Viral dynamic models (e.g., [1,3,7,11]) consider the within-host dynamics independent of the interaction at the population level, whereas epidemiological models of population dynamics (e.g., [1,9] and references therein) consider the interaction between susceptible and infected hosts without an explicit link to the viral dynamics within the hosts. There are, however, questions that can only be studied by using models that explicitly link the two processes. Such questions include: (i) How does the within-host dynamics influence the transmission of a pathogen from individual to individual? (ii) What is the effect of population dynamics of disease transmission on the viral dynamics at the individual level? (iii) Will the model predictions in terms of the virulence and basic reproduction number of the pathogen be altered if the two process are dynamically linked [5]? Gilchrist and Sasakiz [6] have used a nested model to evaluate the direction of natural selection (in the study of evolution of virulence) at the within- and between-host levels. In this nested model, the within-host system is independent of the transmission dynamics at the population level.

In this paper, we propose a framework that explicitly links the epidemiological and immunological dynamics through an environmental compartment. Our approach is based on the idea of separating biological time scales, a fast time scale associated with the within-host dynamics, an intermediate time scale associated with the epidemiological process, and a slow time scale associated with the environment. In a simpler case the processes associated with epidemiology and environment can be merged. We demonstrate our framework by using as a simplified model system for the infection by *Toxoplasma gondii*. *Toxoplasma* is an infectious disease for which contamination of the environment plays a major and determinant role in transmission. One of the advantages of this modeling approach (relative to other approaches for modeling within-host between-host transmission processes) is that the explicit linkage between the two processes can be established through environmental contamination, and it allows to postulate an 'inoculum' size related to the degree of infectiousness of the contaminated environment. To the best of our knowledge, all existing models that attempt to couple immunological and epidemiological dynamics confront the difficult and controversial question as to how to model the influence of the epidemiological dynamics on the within-host cellular infection. We propose, as a first step in that direction, the study of infectious diseases where the environmental component is important.

* Corresponding author.
E-mail addresses: zfeng@math.purdue.edu (Z. Feng), jx.velasco@gmail.com (J. Velasco-Hernandez), bretasa@gmail.com (B. Tapia-Santos).

0025-5564/$ - see front matter © 2012 Elsevier Inc. All rights reserved.
http://dx.doi.org/10.1016/j.mbs.2012.09.004

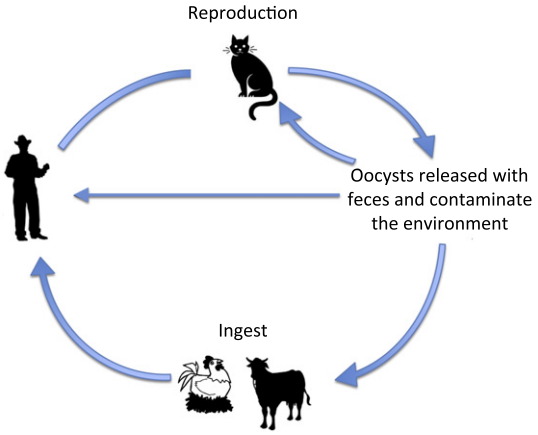

Fig. 1. A depiction of the *T. gondii* life cycle relevant to the model presented here.

2. Key aspects of *Toxoplasma gondii* life cycle

For more information about the complex life cycle of *Toxoplasma gondii*, the recently published studies [8,10] provide detailed descriptions relevant to mathematical modeling of *Toxoplasma*. Only a brief description is provided in this section. *Toxoplasma gondii* is an obligate intracellular parasite that can infect all warm-blooded vertebrates, including mammals and birds. Infections in humans reaches 30% and can cause encephalitis in immunocompromised persons such as AIDS patients or recipients of organ transplants. Infection acquired during pregnancy may cause severe damage to the fetus. *T. gondii* has a complex life cycle and a simplified diagram of the cycle is depicted in Fig. 1.

The parasite reproduces sexually in felines. Once a cat becomes infected, it sheds oocysts, which contaminate the environment. These oocysts can be ingested by mammals and birds which then become infected with the parasite [8]. Eating another organism that is infected can also infect the secondary hosts. These are the main facts that will be used in our model below, although the parasite's life cycle within a host is much more complicated. Again, following Sullivan et al. [8] and references therein we know that, within a host, *T. gondii* exists in two stages that can be reached intermittently: bradyzoites and tachyzoites. Bradyzoites are the slow-growing and encysted form, whereas tachyzoites are the fast-replicating parasites, which lead to the acute phase of infection. After cysts are ingested by the host, the cysts are digested and bradyzoites, which are resistant to gastric conditions in the stomach, will subsequently invade the host's epithelial cells and convert into tachyzoites. While most of tachyzoites in immunocompetent hosts are eliminated by the innate and adaptive immune responses, some tachyzoites differentiate into the dormant bradyzoite stage inside host cells. The differentiation of tachyzoites into the bradyzoite stage plays an essential role in the development of tissue cysts, which allows life-long persistence of the parasites in the host. Reactivation of bradyzoites back to tachyzoites can lead to life threatening infection.

3. The model

One of the main features of the life cycle of *Toxoplasma* is that it comprises three distinct time scales. The first time scale is the one associated with the infection between individuals, that is, the epidemiological time scale that takes place according to the contacts of cats and infectious agents or reservoirs. The second time scale is the one at the individual level. It is related to the reproductive cycle within the host and its interaction with the host immune system that ultimately results either in the clearance of *Toxoplasma* from the host system or in disease. The third time scale is the environmental time scale. *Toxoplasma* is essentially an environmentally-driven disease. Oocysts may survive in the environment for a long time and, a most important factor for our modeling strategy and theoretical framework, infection of an animal reservoir depends on the level or amount of contamination. As in many other diseases that are transmitted through the environment, the size of the inoculum is important in the likelihood of infection in any given host [4].

We have previously studied models that consider interactions between epidemiological and cell-virus dynamics [5]. The main difficulty that we encountered was how to link the epidemiological dynamics to the viral proliferation dynamics within the host. The other direction, i.e., linking the within-host dynamics to the epidemiological dynamics, can be established through the concept of virulence since this factor is directly related to infectiousness [2]. The epidemiological process takes place on a time scale of weeks or months, whereas the disease onset may take place on a scale of days and the actual infection process can occur within hours of acquiring the pathogen. This faster time scale is the main reason for the difficulties mentioned above when linking these processes. The environmental connection for diseases such as *Toxoplasma* allows us to bypass this problem as the infection process is delayed by the pathogen's residence in a quiescent state in the environment.

Although the work presented in this paper is motivated by modeling the biological process of *Toxoplasma*, we demonstrate our framework based on the diagram illustrated in Fig. 1, which omits some of the complexities in the life cycle of *Toxoplasma gondii* including the prey–predator interaction (e.g, rats-cats interaction) that can be involved in the disease transmission process. Thus, the model is merely a caricature of *Toxoplasma* infection. However, the proposed modeling framework allows us to analyze the between-host and within-host dynamics in a way that is more transparent than those presented in [5], at least from the conceptual point of view.

The between-host dynamics is governed by the *SI* system

$$\begin{aligned} \frac{dS}{dt} &= \mu N - \lambda ES - \mu S, \\ \frac{dI}{dt} &= \lambda ES - \mu I, \\ N &= S + I. \end{aligned} \tag{1}$$

The variables $S = S(t)$ and $I = I(t)$ represent the numbers of susceptible and infectious individuals, respectively, at time t. The parameter μ is the per-capita host natural mortality rate, which is assumed to be the same as the per-capita birth rate so that the total population size N remains constant for all time t. The parameter λ denotes the per-capita infection rate of hosts in a contaminated environment, and $E = E(t)$ denotes the level of environment contamination at time t, or the concentration of oocysts per unit area or volume of a region being considered ($0 \leqslant E \leqslant 1$). This level of contamination is dependent of the number of infected hosts (I) and the average parasite load (V) within the host as described by the equation

$$\frac{dE}{dt} = \theta IV(1 - E) - \gamma E, \tag{2}$$

where θ is the rate of contamination and γ is the clearance rate.

For the within-host dynamics, the sub-system reads

$$\begin{aligned} \frac{dT}{dt} &= \Lambda - kVT - mT, \\ \frac{dT^*}{dt} &= kVT - (m + d)T^*, \\ \frac{dV}{dt} &= g(E) + pT^* - cV. \end{aligned} \tag{3}$$

The variables T, T^*, and V represent the density of healthy cells, infected cells, and parasite load, respectively. The parameter k denotes the per-capita infection rate of cells; m and d are the per capita background mortality and infection-induced mortality rates of cells, respectively; p is the parasite reproduction rate by an infected cell; and c is the within-host mortality rate of parasites. The function $g(E)$ represents the rate at which an average host is inoculated.

In order to link the environmental contamination with the infection process at the individual level, we must postulate a mechanism. In this work we assume that environmental contamination is measured by or related to the concentration of pathogenic forms living in the environment, and that hosts acquire infection by ingesting contaminated food (which exists in the environment). The function g expresses the fact that if the environmental contamination is high then the inoculum (the average per capita concentration of pathogen's infectious forms introduced into a given host) is also high. These biological considerations suggest that the function g should have the following properties:

$$g(E) \geqslant 0, \quad g(0) = 0, \quad g'(E) > 0. \tag{4}$$

Although in general the function g may reach a saturation level, we consider here a simpler linear form as our aim is to illustrate the framework of linking within-and between-host dynamics. A saturating "functional response" will be explored with detail in further studies. Thus, we consider the linear form

$$g(E) = aE, \tag{5}$$

where a is a positive constant.

We point out that the inclusion of the inoculation $g(E)$ is the key for linking the within-host dynamics to the between-host dynamics. In directly-transmitted diseases, this function is of the form pT and is directly associated with the target cells that the pathogen infects, whereas in the current model the link is established though the external variable E.

4. Model analysis

As pointed in the previous section, an important biological feature of this coupled system is that the within-host dynamics occurs on a faster time scale than the dynamics of the between-host and the environment. This multiple time-scale allows us to study the mathematical properties of the model by analyzing the fast- and slow-systems determined by the two time scales.

4.1. The fast system

The subsystem for the within-host dynamics (3) can be considered as the fast system in which the variable E is treated as a constant (i.e., it is not changing with time on the fast time scale). In the simpler case when $g(E) = 0$, the system always has the infection-free equilibrium $U_0 = (T_0, T_0^*, V_0)$ where $T_0 = \Lambda/m,\ T_0^* = 0,\ V_0 = 0$. The system has no infection-free equilibrium when $g(E) > 0$.

Let $\mathcal{R}_v(E)$ denote the within-host reproduction number, which is a function of the environmental contamination level, and let

$$\mathcal{R}_{v0} = \mathcal{R}_v(0).$$

The formula for $\mathcal{R}_v(E)$ when $E > 0$ will be specified later. It is easy to derive that

$$\mathcal{R}_{v0} = \frac{T_0 kp}{c(m+d)}. \tag{6}$$

The biological meaning of $\mathcal{R}_{v0}$ is clear. T_0 is the total target cells in the absence of parasite; p/c is the net virion production per cell before clearance, and $k/(m+d)$ is the infection rate during an average timespan of an infected cell. Thus, $\mathcal{R}_{v0}$ represents the baseline within-host reproduction number. We show in Section 4.1.1 that U_0 is l.a.s. if $\mathcal{R}_{v0} < 1$ and unstable if $\mathcal{R}_{v0} > 1$.

Consider the case when $g(E) > 0$. Let $\tilde{U}(E) = \left(\tilde{T}(E), \tilde{T}^*(E), \tilde{V}(E)\right)$ denote a nontrivial equilibrium (i.e., $\tilde{T}^*(E) > 0, \tilde{V}(E) > 0$). Then

$$\tilde{V}(E) = \frac{1}{c}\left(g(E) + p\tilde{T}^*(E)\right), \quad \tilde{T}^*(E) = \frac{m}{m+d}(T_0 - \tilde{T}(E)) \tag{7}$$

and $\tilde{T}(E)$ is a solution of the following quadratic equation:

$$T^2 - a_1 T + a_2 = 0, \tag{8}$$

where

$$\begin{aligned} a_1 &= \tfrac{g(E)[m+d]}{pm} + T_0\left[1 + \tfrac{1}{\mathcal{R}_{v0}}\right] > 0, \\ a_2 &= \tfrac{T_0^2}{\mathcal{R}_{v0}} > 0. \end{aligned} \tag{9}$$

The discriminant of the Eq. (8) is given by

$$\begin{aligned} a_1^2 - 4a_2 &= \left(\frac{g(E)[m+d]}{pm} + T_0\left[1 + \frac{1}{\mathcal{R}_{v0}}\right]\right)^2 - \frac{4T_0^2}{\mathcal{R}_{v0}} \\ &\geqslant T_0^2\left[1 + \frac{1}{\mathcal{R}_{v0}}\right]^2 - \frac{4T_0^2}{\mathcal{R}_{v0}} = T_0^2\left[1 - \frac{1}{\mathcal{R}_{v0}}\right]^2 \geqslant 0. \end{aligned}$$

Thus, (8) has two positive real solutions given by

$$\tilde{T}_{\pm}(E) = \frac{1}{2}\left(a_1 \pm \sqrt{a_1^2 - 4a_2}\right). \tag{10}$$

Note that $a_1'(E) = g'(E)(m+d)/(pm) > 0$ and that

$$\tilde{T}_{\pm}'(E) = \frac{1}{2}a_1'(E)\left(1 \pm \frac{a_1}{\sqrt{a_1^2 - 4a_2}}\right).$$

From $a_2 > 0$ and $a_1'(E) > 0$ we know that

$$\tilde{T}_{+}'(E) > 0, \quad \tilde{T}_{-}'(E) < 0. \tag{11}$$

Note also that

$$\tilde{T}_{+}(0) = \begin{cases} T_0 & \text{if } \mathcal{R}_{v0} \geqslant 1, \\ T_0/\mathcal{R}_{v0} & \text{if } \mathcal{R}_{v0} < 1 \end{cases} \tag{12}$$

and

$$\tilde{T}_{-}(0) = \begin{cases} T_0/\mathcal{R}_{v0} & \text{if } \mathcal{R}_{v0} > 1, \\ T_0 & \text{if } \mathcal{R}_{v0} \leqslant 1. \end{cases} \tag{13}$$

Let $\tilde{U}_{\pm}(E)$ denote the nontrivial equilibria corresponding to $\tilde{T}_{\pm}(E)$. From $\tilde{T}_{+}'(E) > 0$ (see (11)) and $\tilde{T}_{+}(0) \geqslant T_0$ (see (12)) we know that $\tilde{T}_{+}(E) > T_0$ for all $E > 0$. But $\tilde{T}_{+}(E) \leqslant T_0$; and thus, $\tilde{U}_{+}(E)$ does not exist. From (11) and (13) we know that $\tilde{U}_{-}(E)$ exists when $\mathcal{R}_{v0} > 1$ and it coincides with U_0 when $\mathcal{R}_{v0} \leqslant 1$

The existence condition for $\tilde{U}_{-}(E)$ motivates the following definition for $\mathcal{R}_v(E)$ in the case of $E > 0$

$$\mathcal{R}_v(E) =: \frac{T_0}{\tilde{T}_{-}(E)}, \tag{14}$$

where $\tilde{T}_{-}(E)$ is given in (10).

Let $\tilde{U}_{-}(E) = (\tilde{T}_{-}(E), \tilde{T}_{-}^*(E), \tilde{V}_{-}(E))$ where $\tilde{T}_{-}^*(E)$ and $\tilde{V}_{-}(E)$ are given by (7) in which $\tilde{T}(E)$ is replaced by $\tilde{T}_{-}(E)$. Then, we have obtained the following result.

Result 1. Let $g(E) > 0$ and let $\mathcal{R}_v(E)$ be defined in (14).

(i) $\mathcal{R}_v(E)$ is an increasing function of E.
(ii) The fast system has a unique nontrivial equilibrium $\tilde{U}_{-}(E)$ if and only if $\mathcal{R}_{v0} > 1$.

Since $\mathcal{R}_{v0}$ does not depend on E, the influence of E on $\mathcal{R}_v(E)$ and on $\tilde{T}_-(E)$ can be dependent on the magnitude of $\mathcal{R}_{v0}$. Such a dependence is illustrated in Fig. 2. This figure plots the curves $\mathcal{R}_v(E)$ and $\tilde{T}_-(E)$ for two different $\mathcal{R}_{v0}$ values, one with $\mathcal{R}_{v0} > 1$ (the left figure) and the other with $\mathcal{R}_{v0} < 1$ (the right figure). We observe that while $\tilde{T}_-(E)$ is more sensitive to E in the case when $\mathcal{R}_{v0} < 1$ than in the case when $\mathcal{R}_v(0) > 1, \mathcal{R}_v(E)$ is more sensitive to changes in E when $\mathcal{R}_{v0} > 1$. In this figure, we have used a linear function for $g(E) = aE$ where a is a constant and, for demonstration purposes, her parameter values used are $\Lambda = 5000,\ m = 0.31,\ d = 0.1,\ p = 10^4,\ c = 20,\ a = 2\times 10^7$. The two $\mathcal{R}_{v0}$ values used in the two plots are determined by using different k values (e.g., $k = 10^{-7}$ for $\mathcal{R}_{v0} = 2$).

Fig. 3 demonstrates the dependence of the density of infected T cells at the nontrivial equilibrium, $\tilde{T}^*_-$, on both E and $\mathcal{R}_v(0)$. We observe in this figure that $\tilde{T}^*_-$ is more sensitive to changes in E when $\mathcal{R}_v(0)$ is small, and it is more sensitive to changes in $\mathcal{R}_v(0)$ when E is low. In this figure, the function $g(E)$ and other parameter values are chosen to be the same as in Fig. 2.

4.1.1. Stability of the infection-free equilibrium U_0

The Jacobian matrix at $\tilde{U}_0 = (\frac{\Lambda}{m}, 0, 0)$ has one negative eigenvalue $-m$ and two other eigenvalues x given by the equation

$$x^2 + (m + d + c)x + c(m + d) - kpT_0 = 0.$$

It is easy to show that U_0 is locally asymptotically stable (l.a.s.) if $\mathcal{R}_{v0} < 1$, and unstable if $\mathcal{R}_{v0} > 1$.

4.1.2. Stability of the endemic equilibrium $\tilde{U}_-(E)$

The Jacobian matrix at $\tilde{U}_-(E)$ is given by

$$J(E) = \begin{pmatrix} -\frac{\Lambda}{\tilde{T}_-(E)} & 0 & -k\tilde{T}_-(E) \\ \frac{\Lambda}{\tilde{T}_-(E)} - m & -(m+d) & k\tilde{T}_-(E) \\ 0 & p & -c \end{pmatrix}.$$

The characteristic equation is

$$x^3 + B_2x^2 + B_1x + B_0 = 0, \tag{15}$$

where

$$B_0 = mc(m + d)\left[\mathcal{R}_v(E) - \frac{\mathcal{R}_{v0}}{\mathcal{R}_v(E)}\right],$$

$$B_1 = m(c + m + d)\mathcal{R}_v(E) + c(m + d)\left[1 - \frac{\mathcal{R}_{v0}}{\mathcal{R}_v(E)}\right],$$

$$B_2 = c + m + d + m\mathcal{R}_v(E)$$

and $\mathcal{R}_{v0}$ and $\mathcal{R}_v(E)$ are given by (6) and (14), respectively. Recall that $\mathcal{R}_v(E)$ increases with E and that $\tilde{U}_-(E)$ exists only when $\mathcal{R}_{v0} > 1$. Thus, B_0, B_1 and B_2 are all positive numbers. Note that $B_0 < mc(m + d)\mathcal{R}_v(E)$. Note also that $B_1 > m(m + d)\mathcal{R}_v(E)$ and $B_2 > c$; and thus,

$$B_1B_2 > mc(m + d)\mathcal{R}_v(E) > B_0.$$

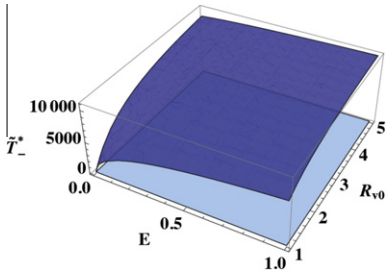

Fig. 3. Plot of $\tilde{T}^*_-$ as a function of $\mathcal{R}_{v0}$ and E. It illustrates that the influence of E on $\tilde{T}^*_-$ is more significant when $\mathcal{R}_{v0}$ is relatively low.

Using the Routh–Hurwitz stability criterion we obtain the local stability of $\tilde{U}_-(E)$. Thus, we have proved the following result.

Result 2. U_0 is l.a.s. when $\mathcal{R}_{v0} < 1$ and unstable when $\mathcal{R}_{v0} > 1$. For all $E > 0, \tilde{U}_-(E)$ is always l.a.s. whenever it exists.

Numerical simulations of the full system for the case of $\mathcal{R}_{v0} > 1$ are illustrated in Fig. 4. The solution curves for infected T-cells (T^*) and viruses (V) are shown in (A). We observe that the fast dynamics quickly stabilizes at the interior equilibrium $\tilde{U}_-$.

4.2. The slow system

We consider the epidemiological and environmental variables to be slow variables, which consist of S, I and E. Assume that $\mathcal{R}_v(E) > 1$ so that the fast system is at the stable nontrivial equilibrium $\tilde{U}_-(E) = (\tilde{T}_-(E),\ \tilde{T}*_-(E), \tilde{V}_-(E))$ with

$$\tilde{T}_- = \frac{T_0}{\mathcal{R}_v(E)},\quad \tilde{V}_- = \frac{1}{c}\left[g(E) + \frac{p\Lambda}{m+d}\left(1 - \frac{1}{\mathcal{R}_v(E)}\right)\right],$$
$$\tilde{T}^*_- = \frac{\Lambda}{m+d}\left(1 - \frac{1}{\mathcal{R}_v(E)}\right) \tag{16}$$

and $\mathcal{R}_v(E)$ is defined in (14) or

$$\mathcal{R}_v(E) = \frac{2T_0}{a_1 - \sqrt{a_1^2 - 4a_2}},$$

where a_1 and a_2 are given in (9).

Since $N = S + I$ remains constant for all time, we can eliminate the S equation and get the following two-dimensional slow system:

$$\dot{I} = \lambda E(N - I) - \mu I,$$
$$\dot{E} = \theta I\tilde{V}_-(E)(1 - E) - \gamma E, \tag{17}$$

where $V = \tilde{V}_-(E)$ is given in (16).

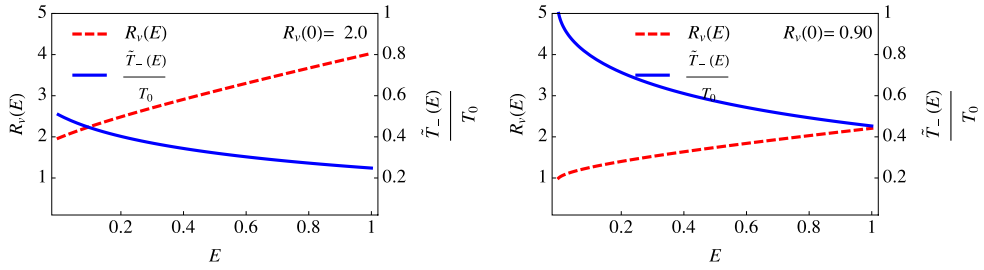

Fig. 2. Plots of the within-host reproduction number $\mathcal{R}_v(E)$ and the proportion of healthy cells at the infection state as functions of environmental contamination level E for different $\mathcal{R}_{v0}$ values. The left figure is for the case when $\mathcal{R}_{v0} = 2 > 1$, in which case $\lim_{E\to 0}\mathcal{R}_v(E) = \mathcal{R}_{v0}$, whereas the figure on the right is for the case of $\mathcal{R}_{v0} = 0.9 < 1$, in which case $\lim_{E\to 0}\mathcal{R}_v(E) = 1$.

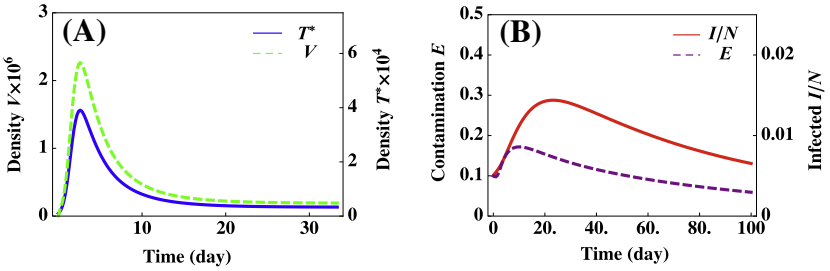

Fig. 4. Simulation results of the full system for the case of $g(E) = aE > 0$. The left figure plots the fast variables T^* and V and the right figure plots the slow variables I and E. We observe that the system stabilizes at the nontrivial equilibrium $\tilde{U}_-$ at $t \to \infty$. The parameter values used are: $\mu = 0.1,\ \lambda = 0.01,\ \gamma = 0.05,\ a = 10^4,\ \theta = 2\times10^{-10},\ \Lambda = 5\times10^3,\ m = 0.3,\ d = 0.1,\ k = 6\times10^{-7},\ p = 5.8\times10^3,\ c = 10^2$.

Notice that the dynamic linkage for the between- and within-host systems is through the environmental contamination variable E. The dependence of E on the within-host dynamics is through the term θVI in the E equation. The two subsystems will be decoupled if V is a constant, in which case we can obtain an isolated reproduction number (i.e., a reproduction number that does not depend on the within-host system) for the between-host system. Without loss of generality, assume that the constant is $V = 1$ (otherwise the scaling constant can be absorbed in the transmission coefficient θ) which leads to the following baseline reproduction number for the between-host dynamics:

$$\mathcal{R}_{h0} =: \frac{\theta\lambda N}{\gamma\mu}. \tag{18}$$

The quantity $\mathcal{R}_{h0}$ plays the role of the classical basic reproduction number for the between-host infection in the absence of the link to the within-host dynamics, as will be shown later in this section.

When the two process are coupled with the fast system being near the equilibrium $\tilde{U}_-(E)$, the variable V in the E equation will be replaced by $\tilde{V}_-(E)$ given in (16). Let $\hat{W} = (\hat{I}, \hat{E})$ denote an interior equilibrium of the slow system, i.e., $\hat{I} > 0$ and $\hat{E} > 0$. Then

$$\hat{I} = \frac{\lambda\hat{E}N}{\lambda\hat{E} + \mu}$$

and $\hat{E}$ satisfies the equation

$$\frac{1-\hat{E}}{c}\left[g(\hat{E}) + \frac{p\Lambda}{m+d}\left(1 - \frac{1}{\mathcal{R}_v(\hat{E})}\right)\right] = \frac{\gamma\hat{E}}{\theta N} + \frac{1}{\mathcal{R}_{h0}}, \tag{19}$$

where N is a constant total population size. Let $F(E)$ and $G(E)$ denote the functions on the left and right hand sides of the Eq. (19), respectively, i.e.,

$$F(E) = \frac{1-E}{c}\left[g(E) + \frac{p\Lambda}{m+d}\left(1 - \frac{1}{\mathcal{R}_v(E)}\right)\right], \quad G(E) = \frac{\gamma E}{\theta N} + \frac{1}{\mathcal{R}_{h0}}. \tag{20}$$

Then, $\hat{E}$ is a solution of the equation $F(E) = G(E)$ with $0 < \hat{E} < 1$. Note that

$$G(0) = \frac{\gamma\mu}{\lambda N\theta} = \frac{1}{\mathcal{R}_{h0}}, \quad G(1) = \frac{\gamma}{\theta N} + \frac{1}{\mathcal{R}_{h0}}, \quad G'(E) = \frac{\gamma}{\theta N} > 0.$$

Thus, $G(E)$ is an increasing function between $1/\mathcal{R}_{h0}$ and $\gamma/(\theta N) + 1/\mathcal{R}_{h0}$. From

$$F(0) = \frac{pmT_0}{c(m+d)}\left(1 - \frac{1}{\mathcal{R}_{v0}}\right), \quad F(1) = 0$$

it follows that there is at least one solution $\hat{E} \in (0,1)$ if $F(0) > G(0)$, which is equivalent to

$$\frac{pmT_0}{c(m+d)}\left(1 - \frac{1}{\mathcal{R}_{v0}}\right)\mathcal{R}_{h0} > 1. \tag{21}$$

It follows from $F(0) > G(0)$ and $F(1) = 0$ that

$$F'(\hat{E}) < 0. \tag{22}$$

The condition (21) motivates the following definition for the reproduction number for the slow (between-host) system when it is coupled with the fast (within-host) system:

$$\mathcal{R}_h =: \frac{pmT_0}{c(m+d)}\left(1 - \frac{1}{\mathcal{R}_{v0}}\right)\mathcal{R}_{h0}. \tag{23}$$

Thus, we have obtained the following result.

Result 3. Let $\mathcal{R}_{v0} > 1$ and let $\mathcal{R}_h$ be defined in (23). Then the slow system has at least one endemic equilibrium $\hat{W} = (\hat{I}, \hat{E})$ if $\mathcal{R}_h > 1$.

Although we were unable to exclude the possibility of multiple endemic equilibria for the slow system, our numerical exploration suggests that for a wide range of parameter values the endemic equilibrium is unique as the curves of $F(E)$ and $G(E)$ have only one intersection for $E \in (0,1)$ (see Fig. 5).

4.2.1. Stability of the endemic equilibrium for the slow system

The Jacobian matrix of the slow system (17) at $\hat{W} = (\hat{I}, \hat{E})$ is given by

$$J(\hat{W}) = \begin{pmatrix} -\lambda\hat{E} - \mu & \lambda(N - \hat{I}) \\ \theta\tilde{V}_-(\hat{E})(1-\hat{E}) & \theta\hat{I}(1-\hat{E})\tilde{V}'_-(\hat{E}) - \theta\hat{I}\tilde{V}_-(\hat{E}) - \gamma \end{pmatrix},$$

or using the notation of $F(E)$ and $G(E)$

$$J(\hat{W}) = \begin{pmatrix} -\mu F(\hat{E})\mathcal{R}_{h0} & \frac{\lambda N}{\mathcal{R}_{h0}G(\hat{E})} \\ \theta G(\hat{E}) & -\frac{\gamma}{F(\hat{E})}\left(F(\hat{E}) - \hat{E}F'(\hat{E})\right) \end{pmatrix}.$$

To obtain the above matrix, the following relations have been used:

$$\overline{V}_-(E) = \frac{F(E)}{1-E} = \frac{G(E)}{1-E}, \quad \theta\hat{I} = \frac{\gamma\hat{E}}{F(\hat{E})}, \quad \lambda\hat{E} = \frac{\lambda\theta N}{\gamma}\left(F(\hat{E}) - \frac{1}{\mathcal{R}_{h0}}\right) = \mu\left(F(\hat{E})\mathcal{R}_{h0} - 1\right).$$

Note that $F(E) > 0$ as $\mathcal{R}_v(E) > \mathcal{R}_{v0} > 1$, and note from (22) that $F'(\hat{E}) < 0$. Thus,

$$K =: F(\hat{E}) - \hat{E}F'(\hat{E}) > 0. \tag{24}$$

The trace and determinant of $J(\hat{W})$ are

$$\mathrm{tr}(J(\hat{W})) = -\mu F(\hat{E})\mathcal{R}_{h0} - \frac{\gamma}{F(\hat{E})}K < 0,$$
$$\det(J(\hat{W})) = \gamma\mu[\mathcal{R}_{h0}K - 1].$$

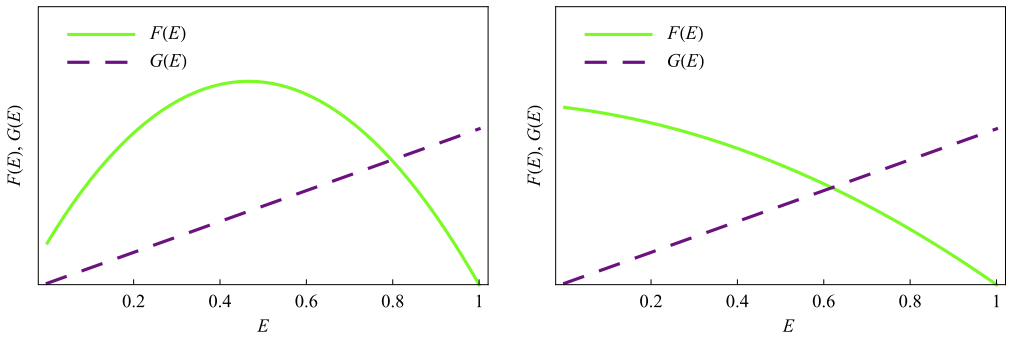

Fig. 5. Plots of the curves determined by $F(E)$ and $G(E)$ whose intersection determines a nontrivial equilibrium of the fast system. In the left plot it shows the case when $F(E)$ is increasing for smaller E and in the right figure F is strictly decreasing. In both cases the curves of F and G have a unique intersection.

Therefore, $\hat{W}$ is l.a.s. if and only if $\det(J(\hat{W})) > 0$. Let

$$\mathcal{R}_{h0}^{*} = \frac{1}{K}, \tag{25}$$

where K is defined in (24). Then the following result holds.

Result 4. An endemic equilibrium $\hat{W}$ of the slow system is l.a.s. if and only if $\mathcal{R}_{h0} > \mathcal{R}_{h0}^{*}$.

Fig. 4(B) illustrates the dynamic behaviors of the slow system. The slow variables I and E are plotted as a function of time and are shown to tend to an endemic equilibrium as t increases. Simulations shown in this figure are computed using the full system. We observe that the convergence to the interior equilibrium of the within-host variables (V and T^{*}) are much faster than the between-host variable (I) and the environment variable (E).

We remark that the stability analysis presented in this section is carried out based on the two decoupled fast and slow systems, with the fast system depending on the slow variables (as constants) and the slow system depending on the steady-state of the fast system. The stability properties from these subsystems can provide insights into the behaviors of the full system by applying the methods in singular perturbation theory. For example, the stability of an endemic equilibrium $\hat{W}$ of the slow system may imply the persistence of the infection at both between- and within-host levels.

5. Conclusions

The dynamics of infectious diseases can be driven by two processes: the epidemiological process occurring at the population level and the immunological process occurring within the host. Both develop on widely different time and spatial scales. Most existing models have considered these two process as decoupled systems or do not link them explicitly. In this work, we developed and analyzed a model that couples explicitly the between- and within-host systems through their connection to a contaminated environment. This coupled system provided new insights into the effect of each of the processes on the other.

Results 1–4 suggest that the existence and stability of equilibrium points of the fast and slow systems are connected to three reproduction numbers: $\mathcal{R}_{v0}, \mathcal{R}_{h0}$ and $\mathcal{R}_{h}$, which are defined in (6), (18) and (23), respectively. These results can be summarized as follows:

(1) For the fast system, the infection-free equilibrium U_0 is l.a.s. $\mathcal{R}_{v0} < 1$. When $\mathcal{R}_{v0} > 1$, U_0 is unstable and a unique interior equilibrium $\tilde{U}_{-}(E)$ exists and is l.a.s.

(2) For the slow system, under the condition that the fast system has the stable interior equilibrium $\tilde{U}_{-}(E)$ (i.e., when $\mathcal{R}_{v0} > 1$), there exists at least one endemic equilibrium $\hat{W}$ if $\mathcal{R}_{h} > 1$.

(3) The endemic equilibrium $\hat{W}$ of the slow system is l.a.s. if and only if $\mathcal{R}_{h0} > \mathcal{R}_{h0}^{*}$.

One of the major findings of this study is the possibility of disease prevalence in the host population even when the isolated between-host reproduction number is less than one. For example, although it is not easy to see from (24) whether $K < 1$ or $K > 1$, for the parameter values used in our simulations (e.g., Figs. 2 and 4) we have $K > 1$, in which case $\mathcal{R}_{h0}^{*} < 1$. Note that $\mathcal{R}_{h0}$ represents the baseline between-host reproduction number. Thus, our result shows that the system can have a stable endemic equilibrium even when $\mathcal{R}_{h0} < 1$. That is, the system may have a backward bifurcation.

The coupled system can be used to determine how the within-host reproduction number ($\mathcal{R}_{v}(E)$) and the infection level of the within-host system ($\tilde{T}(E)$ or $T^{*}(E)$) depend on the environmental contamination E. This is illustrated in Figs. 2 and 3. Particularly, we observe that T^{*} is more sensitive to changes in E when $\mathcal{R}_{v0}$ is small, and that T^{*} is less sensitive to $\mathcal{R}_{v0}$ when the level of environmental contamination is high.

Our model analyses also revealed interesting results about how the within-host dynamics may influence the between-host process. For example, the existence and stability of an interior equilibrium of the full system do not require the baseline between-host reproduction number $\mathcal{R}_{h0}$ to be greater than 1, suggesting the existence of a backward bifurcation (see the Remark in Section 4). This outcome is not likely from either the within-host model alone or from the between-host model alone. The threshold conditions, $\mathcal{R}_{v0} > 1$, $\mathcal{R}_{h} > 1$ and $\mathcal{R}_{h0} > \mathcal{R}_{h0}^{*}$ also provide valuable information on how these processes depend on each other and on the environmental conditions.

Finally, as mentioned earlier, the model considered in this paper is more appropriate for an environmentally-driven infectious disease and the parasite has a similar but simpler life cycle than the case of toxoplasma. This model can be modified to include a predator–prey interaction representing the cats and rats populations that can both be infected. We have began to study a such model and the results will be published elsewhere.

Acknowledgements

We acknowledge funding from the National Institute for Mathematical and Biological Synthesis (NIMBioS) through the National Science Foundation EF-0832-858. We also acknowledge the very fruitful discussions and ideas of all members of the *Toxoplasma*

gondii Working Group that have been taking place at NIMBios since 2010. ZF's research is supported in part by the NSF grant DMS-1022758.

References

[1] R.M. Anderson, R.M. May, Infectious Diseases of Humans, Oxford University Press, 1991.
[2] Daniel Coombs, Michael a Gilchrist, Colleen L Ball, Evaluating the importance of within- and between-host selection pressures on the evolution of chronic pathogens, Theoretical Population Biology 72 (4) (2007) 576.
[3] R.J. De Boer, A.S. Perelson, Target cell limited and immune control models of hiv infection: a comparison, Journal of Theoretical Biology 190 (1998) 201.
[4] P. Ewald, Evolution of Infectious Disease, Oxford University Press, 1993.
[5] Zhilan Feng, Jorge Velasco-Hernandez, Brenda Tapia-Santos, Maria Conceição a. Leite, A model for coupling within-host and between-host dynamics in an infectious disease, Nonlinear Dynamics (2012), http://dx.doi.org/10.1007/s11071-011-0291-0.
[6] Michael A Gilchrist, Akira Sasakiz, Modeling host–parasite coevolution: a nested approach based on mechanistic models, Journal of Theoretical Biology 218 (2002) 289.
[7] M.A. Nowak, R.M. May, Virus Dynamics. Mathematical Principles of Immunology and Virology, Oxford University Press, 2000.
[8] Adam Sullivan, Folashade Augusto, Sharon Bewick, Chunlei Su, Suzanne Lenhart, Xiaopeng Zhao, A mathematical model for within-host Toxoplasma gondii invasion dynamics, submitted for publication.
[9] H.R. Thieme, Mathematics in Population Biology, Princeton University Press, 2003.
[10] Matthew Turner, Suzanne Lenhart, Benjamin Rosenthal, Adam Sullivan, Xiaopeng Zhao, Modeling effective transmission strategies and control of the world's most successful parasite, submitted for publication.
[11] D. Wodarz, Killer Cell Dynamics, Springer-Verlag, 2007.